УДК 621.318.38

Determination of Mechanical Force between two Planar Inductors in the Problem of Electrodynamic Excitation of Seismic Waves

Alexander A. Shchitnikov*
Institute of Engineering Physics and Radio Electronics,
Siberian Federal University,
Kirenskogo, 28, Krasnoyarsk, 660041
Russia

Received 27.03.2014, received in revised form 12.04.2014, accepted 07.05.2014

The paper deals with the problem of mechanical interaction between two planar inductors. The results of experiments and simulations are presented.

Keywords: magnetic induction, inductance, modeling, Ampere's law, magnetic field, circular coil.

Introduction

To generate powerful seismic wave various techniques are used, such as explosives, hydropneumatic, inertial and electric systems. Electrical systems are relatively simple in design and they are easy to control systems. They are classified into three categories: electromagnetic, electrodynamic and inductive-dynamic systems [1, 2]. A common feature of these systems is the presence of at least one inductor to generate a magnetic field. The paper presents a model of the electrodynamic impact excitation of seismic waves. The problem was not considered in scientific literature despite its relevance to the development of modern non-explosive seismic prospecting techniques.

1. Determination of the magnetic field of the coil

Electrodynamic method is based on the Amper's law. The force acting on a current-carrying conductor in a magnetic field is defined by the following formula

$$F = BIL\sin\varphi. \tag{1}$$

Mechanical interaction of two current-carrying loops can be represented as follows: one loop generates a magnetic field which acts on the other loop and vice versa. Thus, the analysis of interaction between two loops is divided into two parts: firstly, one needs to calculate the magnetic field generated by the first loop at the location of the second loop and secondly, one needs to determine the force acting on the second loop. According to the Biot-Savart-Laplace law, the magnetic induction $d\vec{B}$, created by element $d\vec{l}$ of conductor with current I, at point A at a distance $\vec{r}$ from $d\vec{l}$ is

$$d\vec{B} = \frac{\mu_0\mu}{4\pi}\cdot\frac{I[d\vec{l}\cdot\vec{r}]}{r^3}, \tag{2}$$

where $\mu_0 = 4\pi\cdot 10^{-7}\frac{\mathbf{Gn}}{\mathbf{m}}$ is the magnetic constant, μ is the magnetic permeability (for air, $\mu \approx 1,0$). Vector product $[d\vec{l}\cdot\vec{r}]$ defines the direction of vector $d\vec{B}$.

*sheld@inbox.ru

Taking into account that we have N identical loops and integrating over all loop elements, we obtain

$$d\vec{B} = N \cdot \oint_l \frac{\mu_0 \mu}{4\pi} \cdot \frac{I[d\vec{l} \cdot \vec{r}]}{r^3}. \tag{3}$$

A schematic representation of the magnetic field around circular loop is shown in Fig. 1.

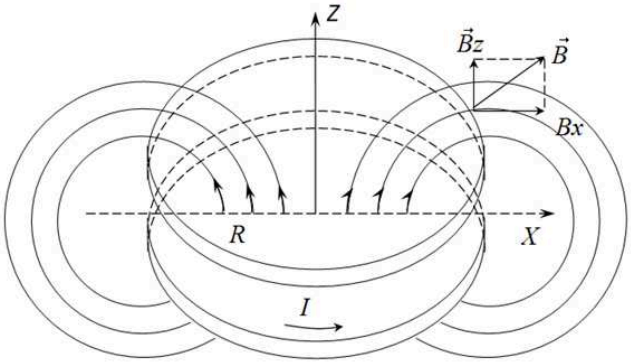

Fig. 1. Magnetic field of the circular loop

It can be seen that the field is symmetric about the loop axis and loop magnetic induction has two components. Component B_Z is perpendicular to the loop plane and component B_X is parallel to the loop plane. Force generated by component B_Z is directed perpendicular to the Z-axis. The force results in the coil extension and it can be neglected. In this model, coils arranged coaxially with the smallest possible distance between them. Component B_X at $x = R$ and $Z = d$ is

$$B_X = N \cdot \frac{\mu_0 \mu I}{4\pi} \cdot \frac{d}{R\sqrt{4R^2 + d^2}} \left[\frac{2R^2 + d^2}{d^2} E - K \right], \tag{4}$$

where R is the coil radius, d is the distance between the centers of coils, E and K are complete elliptic integrals of the first and second kind, respectively. They are defined as follows [3]

$$K = \int_0^{\frac{\pi}{2}} \frac{d\beta}{(1 - k^2 \sin^{-2} \beta)^{0.5}}, \tag{5}$$

$$E = \int_0^{\frac{\pi}{2}} (1 - k^2 \sin^{-2} \beta)^{0.5} d\beta, \tag{6}$$

where $k^2 = \dfrac{4R^2}{4R^2 + d^2}$ and $\beta = \dfrac{\pi - \alpha}{2}$.

To calculate the values of these functions the power series can be used [4]:

$$K = \frac{\pi}{2}(1 + \frac{k^2}{4} + \frac{9}{64}k^4 + \frac{50}{8^3}k^6 + \frac{1225}{4 \cdot 8^4}k^8 + \cdots), \tag{7}$$

$$E = \frac{\pi}{2}(1 - \frac{k^2}{4} - \frac{3}{64}k^4 - \frac{10}{8^3}k^6 - \frac{175}{4 \cdot 8^4}k^8 + \cdots). \tag{8}$$

To increase the intensity of the magnetic field the part of magnetic field lines can be shunted by plate with low magnetic resistance mounted under the magnetic coil. However, this method imposes some restrictions. The maximum saturation induction of the material should not be more than 2 T. In addition, the magnetic permeability of ferromagnetic materials μ is not constant. It strongly depends on the strength of magnetic field H. Typical relationship between μ and H is shown in Fig. 2.

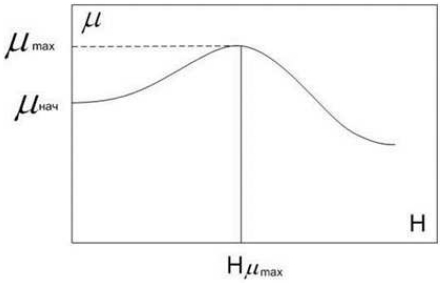

Fig. 2. Dependence of the magnetic permeability on the field intensity

2. Experimental bench

To verify the proposed model the experimental bench has been developed. The bench consists of two coils, 10 mF accumulating capacitor, thyristor and power supply. Two identical coils are used. Each coil consists of 7 turns of wire with rectangular cross-section 3×1 mm wound on the plastic frame of inner diameter 60 mm (Fig. 3).

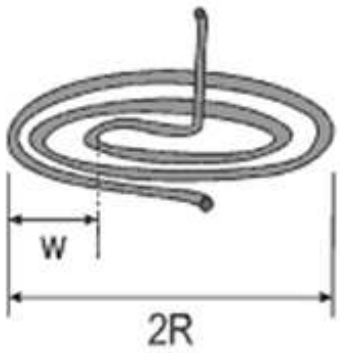

Fig. 3. Schematic representation of the planar coil

Inductance of the planar coils can be calculated as follows [5]

$$L = 33 \cdot 4\pi \cdot 10^{-7} \frac{\mathbf{H}}{\mathbf{m}} \cdot 7^2 \cdot \frac{(40 \cdot 10^{-3}\mathbf{m})^2}{8 \cdot 40 \cdot 10^{-3}\mathbf{m} + 11 \cdot 10 \cdot 10^{-3}\mathbf{m}} = 7.1\mathbf{uH}.$$

The measured value of inductance is 6.7 uH, so the error is about 6 %. Such error is not critical in estimations and confirms the reliability of calculations. One should note that the total inductance of two opposite placed coils is [6]

$$L_{sum} = L_1 + L_2 - 2M, \tag{9}$$

where **M** is the mutual inductance.

Mutual inductance strongly depends on the distance between the coils that is confirmed by the experiment. As one can notice from Fig. 4 the total inductance decreases with the distance between the coils. When the distance is minimal the total inductance is lowered by more than 3 times, reaching 2.2 mH.

Having measured inductance of two opposite placed coils, knowing the capacitance and the initial voltage the force arising on the coil and its duration can be calculated.

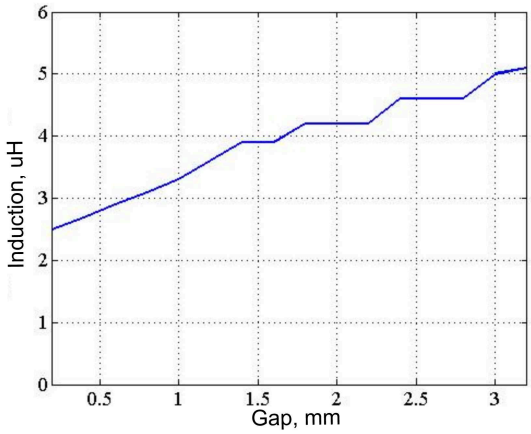

Fig. 4. Dependence of the total inductance from distance

To obtain a model diagram of currents and voltage we simulate the transient processes with the use of the program LTSpice [7].

The model is to be compared with the experiment so it is necessary to take into account non-ideality of elements. The DC resistance of wire coils depends on the material from which the conductors are made, from the area of their cross section and length

$$R = \frac{1.72 \cdot 10^{-8}\mathbf{Ohms} \cdot \mathbf{m} \cdot 3.2\mathbf{m}}{3\mathbf{mm}^2} = 20\mathbf{mOhms}.$$

The DC resistance of the coil is 20 milliohms. One should add 10 milliohms to this value to account for the internal resistance of the open thyristor and resistance of connecting wires. The result of simulation is shown in Fig. 5 where red line shows the capacitor voltage and blue line shows the current flowing through the coils.

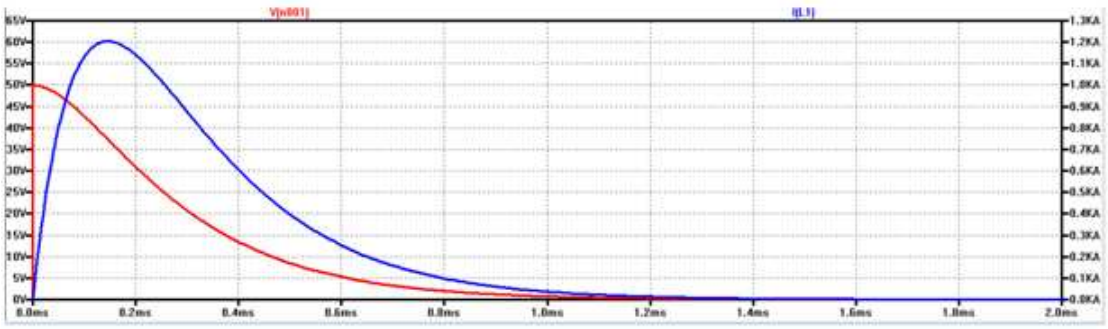

Fig. 5. Diagrams of voltage and current in the circuit

The tests conducted using laboratory bench Fig. 6 show that the maximum value of the current is about 800 A (Fig. 7). The current reaches the value of 200 A almost immediately. It means that the system has active losses. The effect disappears with increasing the distance between coils. This can be explained by interference between wires of nearby coils. In reality, the loss in the wires depends not only on the DC resistance. The skin effect and the so-called proximity effect also contribute to the losses [5].

The skin effect reduces the effective area of cross-section of the conductor because the high

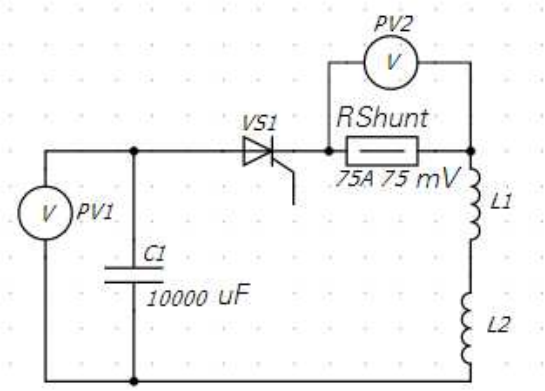

Fig. 6. Schematic diagram of the experiment

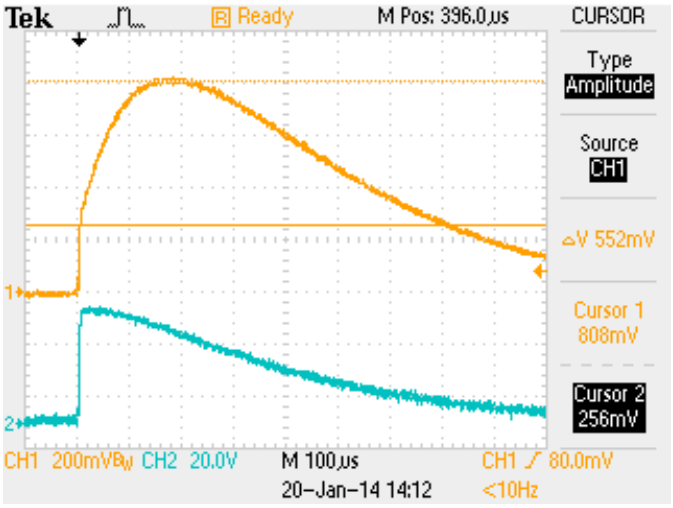

Fig. 7. Current and voltage oscillograms

frequency alternating current flows predominantly in the surface layer. The skin depth is

$$\delta_i = \sqrt{\frac{2 \cdot 1.72 \cdot 10^{-8}\mathbf{Ом} \cdot \mathbf{мм} \cdot 6.7 \cdot 10^{-3}\mathbf{Гц}}{4 \cdot \pi \cdot 10^{-7}\frac{\mathbf{Гн}}{\mathbf{м}}}} = 0.8\mathbf{мм}\,.$$

The influence of the skin effect can be neglected because the size of wire is 3×1 mm.

The proximity effect implies that eddy currents are formed in a wire loop under the influence of the magnetic field from the neighboring loops of the wire in the coil. Obviously, the proximity effect further increases the alternating current impedance. The effect decreases with increasing the steps between the turns. One should note that the proximity effect and the skin effect are caused by the interaction of high frequency current and magnetic field.

The electromagnetic field associated with the high frequency inductors is very complex, so there are no simple relations to calculate the proximity effect in an arbitrary radio frequency coil. One can employ computer simulation with the use of finite element method based software, such as COMSOL Multiphysics, FEMM, ANSYS, etc. To simplify the calculations some pseudoanalytic calculation methods are used. They are based on tables derived from experimental

data.

Table (Fig. 8) presenting the dependence of the proximity effect factor on the ratio of length to diameter of a coil (l/D) and on the ratio of winding pitch to wire diameter (p/d) can be found in [6].

p/d → / l/D ↓	1	1.111	1.25	1.429	1.667	2	2.5	3.333	5	10
0	**5.31**	**3.73**	**2.74**	**2.12**	**1.74**	**1.44**	**1.20**	1.16	1.07	1.02
0.2	**5.45**	**3.84**	**2.83**	**2.20**	**1.77**	**1.48**	**1.29**	1.19	1.08	1.02
0.4	**5.65**	**3.99**	**2.97**	**2.28**	**1.83**	**1.54**	**1.33**	1.21	1.08	1.03
0.6	**5.80**	**4.11**	**3.10**	**2.38**	**1.89**	**1.60**	**1.38**	1.22	1.10	1.03
0.8	**5.80**	**4.17**	**3.20**	**2.44**	**1.92**	**1.64**	**1.42**	1.23	1.10	1.03
1	**5.55**	**4.10**	**3.17**	**2.47**	**1.94**	**1.67**	**1.45**	1.24	1.10	1.03
2	**4.10**	**3.36**	**2.74**	**2.32**	**1.98**	**1.74**	**1.50**	1.28	1.13	1.04
4	**3.54**	**3.05**	**2.60**	**2.27**	**2.01**	**1.78**	**1.54**	1.32	1.15	1.04
6	**3.31**	**2.92**	**2.60**	**2.29**	**2.03**	**1.80**	**1.56**	1.34	1.16	1.04
8	3.20	2.90	2.62	2.34	2.08	1.81	1.57	1.34	1.165	1.04
10	3.23	2.93	2.65	2.27	2.10	1.83	1.58	1.35	1.17	1.04
∞	3.41	3.11	2.815	2.51	2.22	1.93	1.65	1.395	1.19	1.05

Fig. 8.

The ratio of length to diameter of the investigated coils (l/D) can be taken close to zero and the ratio of winding pitch to wire diameter (p/d) = 1.5. Then the proximity effect factor is found to be 2.12. Therefore, the real value of the coil resistance becomes 50 milliohms.

3. Estimation of the mechanical interaction

To estimate the mechanical interaction between two oppositely placed coils the experimental setup shown in Fig. 9 has been used.

The purpose of the experiment is to measure the displacement of the moving coil H_{max} under the action of Ampere's force. If the duration of the force action and mass of the coil are known then the force acting on the coil can be determined. The friction force is not taken into account in this experiment. The magnetic field is assumed to be homogeneous.

Magnetically conductive plates (1) made from iron, ferrite and steel were used in experiments. The results of experiments are shown in Tab. 1.

Table 1.

Material of magnetically conductive plate	H_{max},mm
without plate	44
iron	55
ferrite	55
steel	57

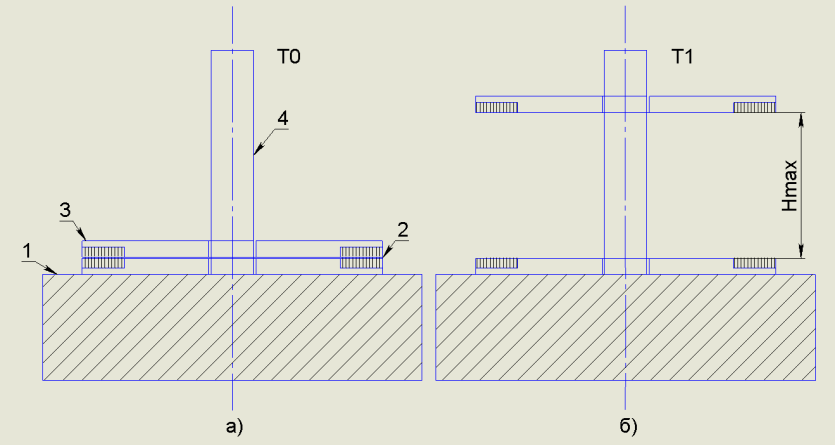

Fig. 9. Experimental setup: 1 — plate with low magnetic resistance; 2 — magnetization coil; 3 — moving coil; 4 — guiding rail

To confirm the above estimation the numerical calculation of coil motion based on current oscillogram given in Fig. 7 is used Tab. 2.

Table 2. Initial data used in calculation

Parameter	Value
Weight of coil	92 g
Elevation of coil	44 mm
Wires length	1.6 m
Number of turns	7
The average radius of turns	35 mm
The distance between the coils	1 mm

The moving coil is raised through a height less than 50 mm under the action of Amper's force. Taking into account the data for the total inductance shown in Fig. 4, the change in coil parameters is negligibly small.

The magnetic induction in the moving coil against time can be calculated with the use of expression (4). To do this one needs to know the time dependence of current and the coil dimensions. The dependence of the magnetic field on time is shown in Fig. 10.

The force acting on the coil is calculated by relation (1). The dependence of the force on time is shown in Fig. 11.

The dependence of the speed of the moving coil on time is shown in Fig. 12.

The equation of the vertical motion of a body under the influence of gravity with nonzero initial velocity is

$$S = V_0 t - \frac{gt^2}{2}. \tag{10}$$

The dependence of the elevation of the moving coil on time is shown in Fig. 13.

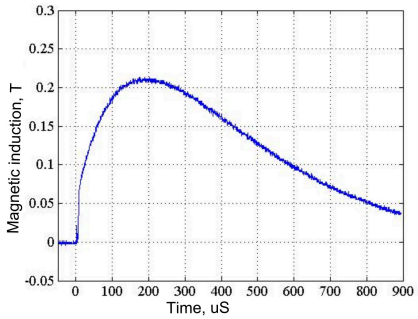

Fig. 10. Dependence of the magnetic field on time

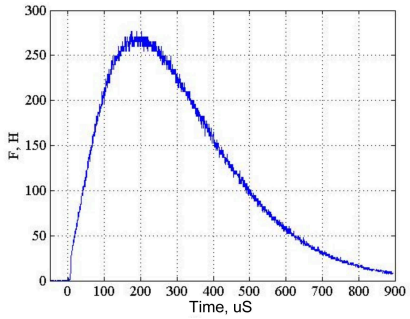

Fig. 11. Dependence of the Ampere force on time

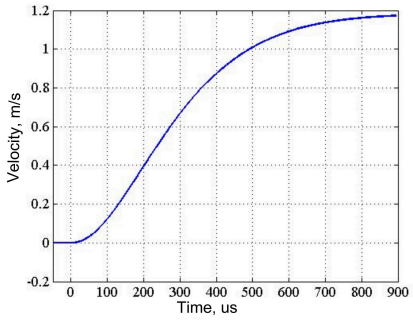

Fig. 12. Dependence of the coil speed on time

Conclusion

The paper assesses the possibility of creating a mechanical force with the use of two opposite placed planar coils. The disadvantage of the experimental setup is a low Q factor of the system. In consequence of this feature the smooth decrease of the current is observed and the action of mechanical energy is spread over time. To create more sharp pulse it is necessary to increase the value of inductance and reduce ohmic losses. To reduce losses in conductors one can increase the wire cross section but a more perspective solution is to use multistrand wires. The discrepancy between the simulation results and experiments is explained by the laboratory conditions of bench construction and by the fact that friction force and the weight of the power supply conductors

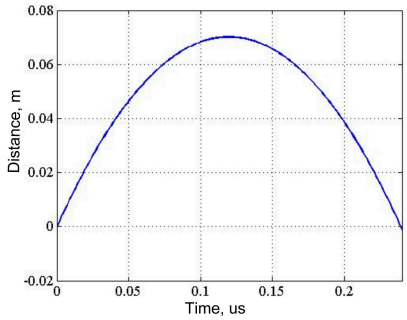

Fig. 13. Dependence of the elevation of the coil on time

has not been taken into account. Rather weak influence of the magnetically conductive plate on the experimental results shown in Tab. 1 can be explained by an attractive force that appears between the magnetically conductive plate and moving coil where the coil plays the role of an electromagnet. This force is inversely proportional to the distance and it is not considered in this paper.

References

[1] M.B.Shneerson, A.M.Lungin, Non-explosive sources of seismic vibrations, Nedra, Moscow, 1992 (in Russian).

[2] V.A.Detkov, V.V.Slabko, G.Ya.Shaidurov, The Possibility of Creation of Rotary-Type Source of Seismic Transverse Waves with Electromagnetic Excitation, Siberian Federal University. Engineering & Technologies, 2013 (in Russian).

[3] A.I.Slobodenuk, Physics, BGU, 2001 (in Russian).

[4] K.S.Dimerchan, L.R.Neyman, Theoretical Foundations of Electrical Engineering. ed.5, Piter, 2009 (in Russian).

[5] D.W.Knight, An introduction to the art of Solenoid Inductance Calculation With emphasis on radio-frequency application. ($http://www.g3ynh.info/zdocs/magnetics/part_1.html$)

[6] R.G.Medhurst, HF resistance and self-capacitance of single-layer solenoids, Wireless Engineer, 1947.

[7] U.N.Sohor, Modelling in the LTSpice/SwCAD//Pskov, 2008 (in Russian).

Оценка силового взаимодействия двух плоских индукционных катушек в задачах создания электродинамических источников сейсмических волн

Александр А. Щитников

Приведены расчеты механического взаимодействия двух встречно включенных плоских катушек индуктивности. Проведено моделирование и эксперименты.

Ключевые слова: индукция магнитного поля, индуктивность, моделирование, сила ампера, магнитное поле кругового витка.